Progress of Theoretical Physics, Vol. 116, No. 1, July 2006

Liquid-Gas Instability and Superfluidity in Nuclear Matter

Masayuki MATSUZAKI*)

Department of Physics, Graduate School of Sciences, Kyushu University, Fukuoka 812-8581, Japan
and
*Department of Physics, Fukuoka University of Education, Munakata 811-4192, Japan***)

(Received May 1, 2006)

We study effects of medium polarization on superfluidity in symmetric nuclear matter in a relativistic formalism. The effect of the liquid-gas instability is emphasized. We examine two types of decomposition of the nucleon propagator, the standard Feynman density and the particle-hole-antiparticle ones. In both cases, the medium polarization effect is determined by a characteristic cancellation among the σ, the longitudinal ω, and the σ-ω mixed polarizations. The instability leads to an increase of the pairing gap. Around the saturation density, which is free from the instability, the medium polarization enhances the pairing gap in the former case and reduces it in the latter. At the lowest density, which is also free from the instability, the gap increases in both cases.

§1. Introduction

Superfluidity in nuclear matter has long been studied, mainly in pure neutron matter, from the point of view of neutron star physics, with regard to such behavior as cooling rates and glitch phenomena.[1] In addition, superfluidity in nuclear matter with a finite Z/N ratio is also becoming of interest as basic information concerning the theory of the structure of finite nuclei, since recent developments in RI-beam experiments have made it possible to study $N \simeq Z$ medium-heavy nuclei and neutron-rich light nuclei.

At present, there are two models used to describe fundamental properties, such as the saturation property of finite-density nuclear many-body system, the non-relativistic and the relativistic models. They are understood as describing observed properties almost equally well. Here we adopt the latter. The origin of quantum hadrodynamics (QHD) can be traced back to Duerr's relativistic nuclear model,[2] which reformulated a non-relativistic field theoretical model of Johnson and Teller.[3] Since Chin and Walecka succeeded in reproducing the saturation property of symmetric nuclear matter within the mean-field approximation,[4–6] not only has QHD evolved beyond the mean-field approximation as a many-body theory, but also its realm of applicability has gradually enlarged from infinite matter to include spherical nuclei, deformed nuclei, and rotating nuclei.[7,8] These successes indicate that the particle-hole channel interaction in QHD is realistic. By contrast, to this time,

*) E-mail: matsuza@fukuoka-edu.ac.jp
**) Permanent address.

relativistic nuclear structure calculations with pairing have been carried out using particle-particle channel interactions borrowed from non-relativistic models, and therefore the particle-particle channel in QHD has not been studied fully, even in infinite matter. Despite its practical successes, this situation is unsatisfactory theoretically. For this reason, in this paper, we attempt to derive an in-medium particle-particle interaction that is consistent with the relativistic mean field (RMF), although only infinite matter can be treated at the present stage.

There have been many non-relativistic studies of pairing in nuclear matter. For the particle-particle interaction entering into the gap equation, many authors have adopted bare interactions, whereas others have adopted renormalized ones, such as G-matrices. Although in the medium, intuitively it seems that renormalized interactions should be used, the following reasons support the use of bare interactions: (1) The Green function formalism leads to a sum of irreducible diagrams,[9),10)] and its lowest order is the bare interaction; (2) the gap equation itself implies a short-range correlation.[1),10)–12)] In general, medium renormalizations are believed to enhance the gap by weakening the short-range repulsion. An interesting exception is the Gogny force. This is known to reproduce the pairing properties given by bare interactions, at least at low densities.[13)] In any case, as the next step, polarization diagrams should be considered. In the non-relativistic framework, there have been many works studying medium polarization effects on superfluidity in neutron matter.[14)–22)] All of them concluded that the medium polarization reduces the pairing gap significantly. A recent *ab initio* calculation,[23)] however, indicates that the polarization effect is weak. Studies of polarization effects on symmetric nuclear matter have just recently begun. Reference 24) reports that the gap *increases* substantially. In the low density limit, Ref. 19) argues that in Fermi systems with four species, the medium polarization enhances the gap.

Symmetric matter has also been studied in the relativistic framework.[25),26)] Both Refs. 25) and 26) report that the vacuum polarization reduces the gap, while the latter reports that the medium polarization enhances the gap. References 26) and 27) argue that the increase of the gap is related to the existence of an instability. This is known as the liquid-gas instability.[28)–30)]

In this paper, we investigate the liquid-gas instability and its effects on superfluidity in symmetric nuclear matter. Results for the case of pure neutron matter are also mentioned briefly. Preliminary results are reported in Ref. 31).

§2. Liquid-gas instability in the relativistic random phase approximation

We begin with the ordinary σ-ω model Lagrangian density,

$$\begin{aligned}\mathcal{L} &= \bar{\psi}(i\gamma_\mu\partial^\mu - M)\psi \\ &\quad + \frac{1}{2}(\partial_\mu\sigma)(\partial^\mu\sigma) - \frac{1}{2}m_\sigma^2\sigma^2 - \frac{1}{4}\Omega_{\mu\nu}\Omega^{\mu\nu} + \frac{1}{2}m_\omega^2\omega_\mu\omega^\mu \\ &\quad + g_\sigma\bar{\psi}\sigma\psi - g_\omega\bar{\psi}\gamma_\mu\omega^\mu\psi\,, \\ \Omega_{\mu\nu} &= \partial_\mu\omega_\nu - \partial_\nu\omega_\mu\,. \end{aligned} \tag{2·1}$$

Here ψ, σ, and ω are the nucleon, the σ meson, and the ω meson fields, respectively. The quantities M, m_σ, and m_ω are their masses, and g_σ and g_ω are the nucleon-meson coupling constants. The relativistic mean field approximation is carried out by replacing the meson fields in the coupled equations of motion by their expectation values, as

$$\begin{aligned} \sigma &\to \langle\sigma\rangle = \sigma_0 \,, \\ \omega_\mu &\to \langle\omega_\mu\rangle = \delta_{\mu 0}\omega_0 \,. \end{aligned} \tag{2·2}$$

Then the nucleon effective mass (Dirac mass) equation is given by

$$\begin{aligned} M^* &= M - g_\sigma \sigma_0 \\ &= M - \frac{g_\sigma^2}{m_\sigma^2}\frac{\lambda}{\pi^2}\int_0^{k_\mathrm{F}} \frac{M^*}{\sqrt{k^2 + M^{*2}}} k^2 dk \,, \end{aligned} \tag{2·3}$$

where the isospin factor λ can take the values 2 and 1 corresponding to symmetric nuclear matter and pure neutron matter, respectively. The Fermi momentum k_F is related to the baryon density ρ_B as

$$\rho_\mathrm{B} = \frac{\lambda}{3\pi^2} k_\mathrm{F}^3 \,. \tag{2·4}$$

The properties of normal fluid, zero temperature matter of a given density are completely determined by the above effective mass equation, (2·3). The so-called saturation curve, or the equation of state, is given by the binding energy per nucleon, $E/A - M = \mathcal{E}/\rho_\mathrm{B} - M$, as a function of ρ_B or k_F. This immediately gives the pressure,

$$P = \rho_\mathrm{B}^2 \frac{\partial}{\partial \rho_\mathrm{B}} \left(\frac{\mathcal{E}}{\rho_\mathrm{B}} \right) . \tag{2·5}$$

The thermodynamic stability of the matter in the liquid phase is expressed by $\partial P/\partial \rho_\mathrm{B} > 0$. Because the ratio of the sound velocity c_s to the light velocity c is given by

$$\frac{c_\mathrm{s}}{c} = \sqrt{\frac{1}{M}\frac{\partial P}{\partial \rho_\mathrm{B}}} \,, \tag{2·6}$$

the condition $(c_\mathrm{s}/c)^2 < 0$ depicted in Fig. 1 indicates the existence of a mechanical instability to the gas phase. In this paper, we adopt $M = 939$ MeV, $m_\sigma = 550$ MeV, $m_\omega = 783$ MeV, $g_\sigma^2 = 91.64$, and $g_\omega^2 = 136.2$.[33)]

Quantum mechanically, the stability of a state is determined by the second variation of the energy with respect to the fields.[28)] This is equivalent to the random phase approximation (RPA). The RPA in the present model, in which the nucleon-nucleon interaction is mediated by mesons, is formulated by calculating the meson propagators that couple to the particle-hole and particle-antiparticle polarizations.[6),29),30),32)] The Dyson equation that determines the RPA propagator D is given by

$$D = D_0 + D_0 \Pi D \tag{2·7}$$

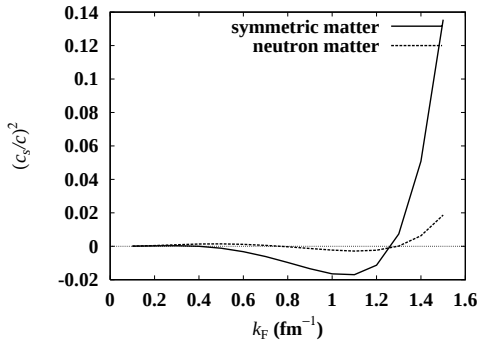

Fig. 1. Squared ratios of the sound velocity to the light velocity as functions of the Fermi momentum.

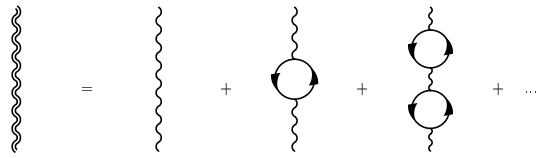

Fig. 2. Feynman diagram representing the RPA meson propagator.

(pictorially described in Fig. 2), where the lowest order propagator,

$$D_0 = \begin{pmatrix} D_0^{\rm S} & 0 \\ 0 & D_{0\mu\nu}^{\rm V} \end{pmatrix}, \tag{2·8}$$

and the polarization insertion,

$$\Pi = \begin{pmatrix} \Pi^{\rm S} & \Pi_\nu^{\rm M} \\ \Pi_\mu^{\rm M} & \Pi_{\mu\nu}^{\rm V} \end{pmatrix}, \tag{2·9}$$

take the form of 5×5 matrices. Their components are given by

$$\begin{aligned} D_0^{\rm S}(q) &= \frac{1}{q^2 - m_\sigma^2 + i\epsilon}\,, \\ D_{0\mu\nu}^{\rm V}(q) &= \left(g_{\mu\nu} - \frac{q_\mu q_\nu}{m_\omega^2}\right) D_0^{\rm V}(q)\,, \quad D_0^{\rm V}(q) = \frac{-1}{q^2 - m_\omega^2 + i\epsilon}\,, \end{aligned} \tag{2·10}$$

and

$$\begin{aligned} \Pi^{\rm S}(q) &= -ig_\sigma^2 \int \frac{d^4k}{(2\pi)^4} {\rm Tr}\big[G(k)G(k+q)\big]\,, \\ \Pi_{\mu\nu}^{\rm V}(q) &= -ig_\omega^2 \int \frac{d^4k}{(2\pi)^4} {\rm Tr}\big[\gamma_\mu G(k)\gamma_\nu G(k+q)\big]\,, \\ \Pi_\mu^{\rm M}(q) &= ig_\sigma g_\omega \int \frac{d^4k}{(2\pi)^4} {\rm Tr}\big[\gamma_\mu G(k)G(k+q)\big]\,. \end{aligned} \tag{2·11}$$

Here, $G(k)$ stands for the nucleon propagator, and the trace, represented by Tr, includes isospin. The quantity $\Pi_\mu^{\rm M}$ stands for the matter-induced σ-ω mixed polarization, in which a σ excites a particle-hole pair, and then it decays into an ω, and

vice versa. Since Eq. (2·7) is formally solved as

$$D = \frac{1}{1 - D_0 \Pi} D_0 \,, \tag{2·12}$$

the zeros of the dielectric function

$$\epsilon = \det\left(1 - D_0 \Pi\right) \tag{2·13}$$

determine collective excitations.

For the present purpose, investigating the instability, only the real parts at zero energy transfer are necessary. Therefore, we set

$$\begin{aligned} D_0^{\mathrm{S}} &= \frac{-1}{|\boldsymbol{q}|^2 + m_\sigma^2} \,, \\ D_0^{\mathrm{V}} &= \frac{1}{|\boldsymbol{q}|^2 + m_\omega^2} \,, \end{aligned} \tag{2·14}$$

and the second term in $D_{0\mu\nu}^{\mathrm{V}}$ drops, because of the baryon number conservation. This conservation law also restricts the non-vanishing components among Π; if we choose the coordinate system as $q = (q^0, 0, 0, |\boldsymbol{q}|)$, only $\Pi^{\mathrm{L}} \equiv \Pi_{00}^{\mathrm{V}} - \Pi_{33}^{\mathrm{V}}$ and $\Pi^{\mathrm{T}} \equiv \Pi_{11}^{\mathrm{V}} = \Pi_{22}^{\mathrm{V}}$ among $\Pi_{\mu\nu}^{\mathrm{V}}$ and $\Pi^0 \equiv \Pi_0^{\mathrm{M}}$ among Π_μ^{M} survive. Note that energy transfer q^0 is set to zero; that is, we employ the instantaneous approximation. After some permutations, $1 - D_0\Pi$ becomes block diagonal, and consequently the dielectric function reduces to

$$\begin{aligned} \epsilon &= \epsilon_{\mathrm{L}} \epsilon_{\mathrm{T}}^2 \,, \\ \epsilon_{\mathrm{L}} &= (1 - D_0^{\mathrm{S}} \Pi^{\mathrm{S}})(1 - D_0^{\mathrm{V}} \Pi^{\mathrm{L}}) - D_0^{\mathrm{S}} D_0^{\mathrm{V}} (\Pi^0)^2 \,, \\ \epsilon_{\mathrm{T}} &= 1 + D_0^{\mathrm{V}} \Pi^{\mathrm{T}} \,. \end{aligned} \tag{2·15}$$

The transverse dielectric function, ϵ_{T}, is always positive in the density region in which superfluidity is realized, whereas the longitudinal one, ϵ_{L}, becomes negative at intermediate densities; this reflects the liquid-gas instability.

In this work, we concentrate on the particle-hole polarization, keeping the correspondence to non-relativistic calculations in mind. We examine two ways to extract the particle-hole polarization, (1) the standard Feynman density (FD) decomposition of $G(k)$ and (2) the particle-hole-antiparticle (pha) decomposition. By definition, the nucleon propagator in the medium is given by

$$\begin{aligned} G(k) &= \frac{1}{2E^*(k)} \Big[(\gamma_\mu K^\mu + M^*) \Big(\frac{1 - \theta(k_{\mathrm{F}} - |\boldsymbol{k}|)}{k^0 - E^*(k) + i\epsilon} + \frac{\theta(k_{\mathrm{F}} - |\boldsymbol{k}|)}{k^0 - E^*(k) - i\epsilon} \Big) \\ &\quad - (\gamma_\mu \tilde{K}^\mu + M^*) \frac{1}{k^0 + E^*(k) - i\epsilon} \Big] \\ &\equiv G_{\mathrm{p}}(k) + G_{\mathrm{h}}(k) + G_{\mathrm{a}}(k) \,, \end{aligned} \tag{2·16}$$

where

$$\begin{aligned} K = \big(E^*(k), \boldsymbol{k}\big), \quad \tilde{K} = \big(-E^*(k), \boldsymbol{k}\big) \,, \\ E^*(k) = \sqrt{\boldsymbol{k}^2 + M^{*\,2}} \,. \end{aligned} \tag{2·17}$$

The first, second, and third terms here represent the propagator of the particle, hole, and antiparticle, respectively. By sorting them with respect to the Heaviside function, another form,

$$G(k) = (\gamma_\mu k^\mu + M^*)\Big(\frac{1}{k^2 - M^{*2} + i\varepsilon} + \frac{i\pi}{E^*(k)}\delta(k^0 - E^*(k))\theta(k_{\rm F} - |\boldsymbol{k}|)\Big)$$
$$\equiv G_{\rm F}(k) + G_{\rm D}(k)\,, \tag{2·18}$$

is obtained. The first and the second terms here are called the Feynman and the density parts, respectively. The former consists of the antiparticle propagation and a part of the particle propagation, while the latter consists of the hole propagation and the other part of the particle propagation. In the standard FD decomposition, the density dependent $G_{\rm F}G_{\rm D} + G_{\rm D}G_{\rm F}$ part in Eq. (2·11) is regarded as the particle-hole polarization. Note that the $G_{\rm D}G_{\rm D}$ part is purely imaginary and therefore is not necessary for the present purpose. In the pha decomposition, the $G_{\rm p}G_{\rm h} + G_{\rm h}G_{\rm p}$ part in Eq. (2·11) represents the particle-hole polarization and this directly corresponds to that in non-relativistic calculations.[34] Explicit expressions of Π are given in Appendix A.

Figure 3 shows the longitudinal dielectric function $\epsilon_{\rm L}$ for the FD and the pha cases in the case of symmetric nuclear matter. At low momentum transfers, $\epsilon_{\rm L}$ becomes negative in both cases. The density range of the instability is nearly the same as that depicted in Fig. 1 for the FD case. This is consistent with the finding in Ref. 28), in which the density range of the instability changes very little, even after inclusion of the vacuum polarization. In the pha case, the instability region shrinks. These results indicate that the liquid-gas instability existing over a wide density range affects the pairing properties calculated using the RPA meson propagator that exhibits instability.

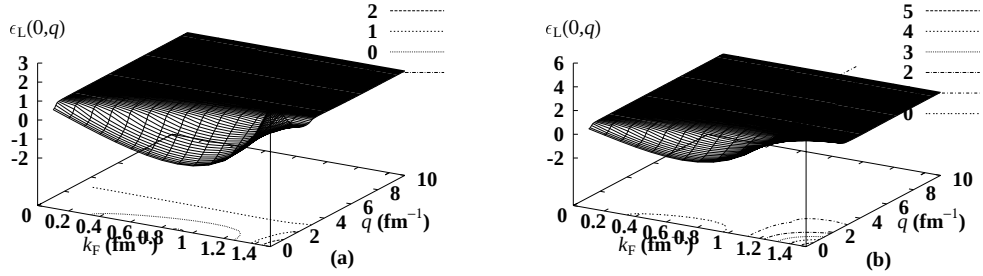

Fig. 3. Longitudinal dielectric functions for symmetric nuclear matter as functions of the Fermi momentum and the momentum transfer: (a) the FD case; (b) the pha case.

§3. Medium polarization effects on superfluidity

The RPA meson propagator is given explicitly by

$$D = \frac{1}{1 - D_0 \Pi} D_0 = \begin{pmatrix} \frac{(1-D_0^{\rm V}\Pi^{\rm L})D_0^{\rm S}}{\epsilon_{\rm L}} & \frac{D_0^{\rm S}D_0^{\rm V}\Pi^0}{\epsilon_{\rm L}} & 0 & 0 & 0 \\ \frac{D_0^{\rm V}D_0^{\rm S}\Pi^0}{\epsilon_{\rm L}} & \frac{(1-D_0^{\rm S}\Pi^{\rm S})D_0^{\rm V}}{\epsilon_{\rm L}} & 0 & 0 & 0 \\ 0 & 0 & \frac{-D_0^{\rm V}}{\epsilon_{\rm T}} & 0 & 0 \\ 0 & 0 & 0 & \frac{-D_0^{\rm V}}{\epsilon_{\rm T}} & 0 \\ 0 & 0 & 0 & 0 & -D_0^{\rm V} \end{pmatrix} . \quad (3\cdot1)$$

This gives the particle-particle channel interaction, which determines superfluidity, as

$$V_{\rm RPA} = \sum_{a,b=-1}^{3} g_a \Gamma_a D^{a,b} g_b \Gamma_b \,,$$
$$g_a = \begin{cases} g_\sigma, \\ -g_\omega, \end{cases} \qquad \Gamma_a = \begin{cases} 1 & : a = -1, \\ \gamma_\mu & : a = \mu. \end{cases} \quad (3\cdot2)$$

The antisymmetrized matrix element of this interaction for the ${}^1S_0$ pairing channel is given by

$$\bar{v}(\boldsymbol{p}, \boldsymbol{k}) = \langle \boldsymbol{p}s', \tilde{\boldsymbol{p}s'} | V_{\rm RPA} | \boldsymbol{k}s, \tilde{\boldsymbol{k}s} \rangle - \langle \boldsymbol{p}s', \tilde{\boldsymbol{p}s'} | V_{\rm RPA} | \tilde{\boldsymbol{k}s}, \boldsymbol{k}s \rangle . \quad (3\cdot3)$$

Here, the argument $|\boldsymbol{q}|$ of D in $V_{\rm RPA}$ is given by $\boldsymbol{q} = \boldsymbol{p} - \boldsymbol{k}$, and the tildes represent the time reversal operation. The pairing gap in relativistic systems can be described in terms of the relativistic Nambu-Gor'kov formalism.[35),36)] In Ref. 36) it was shown that the effect of the coupling to the negative energy states on the Fermi sea pairing is negligible. Ignoring this coupling, the relativistic Nambu-Gor'kov equation reduces to the usual gap equation,[36)]

$$\Delta(p) = -\frac{1}{8\pi^2} \int_0^\infty \bar{v}(p,k) \frac{\Delta(k)}{\sqrt{(E_k - E_{k_{\rm F}})^2 + \Delta^2(k)}} k^2 dk \,, \quad (3\cdot4)$$

after integration with respect to the angle between $\boldsymbol{p}$ and $\boldsymbol{k}$. The effective mass equation (2·3) is slightly modified when superfluidity is realized, becoming

$$M^* = M - \frac{g_\sigma^2}{m_\sigma^2} \frac{\lambda}{\pi^2} \int_0^\infty \frac{M^*}{\sqrt{k^2 + M^{*2}}} v_k^2 k^2 dk \,,$$
$$v_k^2 = \frac{1}{2} \left(1 - \frac{E_k - E_{k_{\rm F}}}{\sqrt{(E_k - E_{k_{\rm F}})^2 + \Delta^2(k)}} \right) . \quad (3\cdot5)$$

Here we have $E_k = E^*(k) + g_\omega \langle \omega_0 \rangle$. Using these equations, we calculate superfluidity in nuclear matter assuming that it is in a pure phase even in the density range in which the liquid-gas instability would appear, as usual. We set the upper bound of the integrations to 20 fm^{-1}.

Here, some discussion about our choice of the interaction is in order. At lowest order (i.e. tree level, in which case we have $D \to D_0$), $V_{\rm RPA}$ reduces to the one-boson exchange (OBE) interaction $V_{\rm OBE}$ given by the RMF vertices (see Fig. 2). It is well known that this OBE interaction gives an unphysically large pairing gap.[35] The reason for this can be traced back to the fact that the RMF vertices were tuned only below the Fermi momentum. In order to treat the higher-order (polarization) effects, this OBE result must first be improved. We accomplish this by introducing a form factor that smoothly modulates the high momentum part of the interaction[37] as follows. Note that the authors of Ref. 26) adopted sudden momentum cutoffs so as to reproduce the virtual state in the T matrix. We argued in Ref. 37) that a sudden cutoff distorts the shape of the short-range pair wave function. (See also Ref. 38) for a sudden momentum cutoff that reproduces the results of a bare interaction in the pairing calculation.) From a general argument, the lowest order in the particle-particle channel interaction that gives pairing should be a bare interaction and the particle-hole channel interaction that determines the medium polarization should be an in-medium one in principle. In the present investigation, however, we calculate the tree and bubble contributions on the same footing, adopting an interaction of in-medium nature, which reproduces the results of the bare interaction at tree level. That is, in a sense, we regard the present RMF-OBE interaction with a form factor as resembling the Gogny force in the non-relativistic pairing calculations.

In order to modulate the high momentum interaction that enters into the pairing calculation, we introduce the form factor

$$f(\boldsymbol{q}^2) = \frac{\Lambda^2}{\Lambda^2 + \boldsymbol{q}^2} \tag{3·6}$$

at each vertex. Other forms were also examined in Ref. 37), but it was found that their effects are very similar. The introduction of the form factor does not affect the mean field (Hartree) part with momentum transfer $\boldsymbol{q} = 0$. The parameter Λ is determined so as to minimize the difference between the pairing properties obtained with the present calculation and those obtained with the RMF+Bonn calculation, which is a hybrid calculation performed by adopting single particle states from the RMF model and the Bonn potential as the pairing interaction. Here we adopt the Bonn-B potential, because this has moderate properties among the available (charge-independent) versions A, B, and C.[39] The pair wave function,

$$\begin{aligned} \phi(k) &= \frac{1}{2}\frac{\Delta(k)}{E_{\rm qp}(k)}\,, \\ E_{\rm qp}(k) &= \sqrt{(E_k - E_{k_{\rm F}})^2 + \Delta^2(k)}\,, \end{aligned} \tag{3·7}$$

is related to the gap at the Fermi surface,

$$\Delta(k_{\rm F}) = -\frac{1}{4\pi^2}\int_0^\infty \bar{v}(k_{\rm F}, k)\phi(k)k^2 dk\,, \tag{3·8}$$

and its derivative determines the coherence length,

$$\xi = \left(\frac{\int_0^\infty |\frac{d\phi}{dk}|^2 k^2 dk}{\int_0^\infty |\phi|^2 k^2 dk} \right)^{\frac{1}{2}} , \tag{3·9}$$

which measures the spatial size of the Cooper pairs. These expressions indicate that $\Delta(k_{\rm F})$ and ξ carry independent information, ϕ and $\frac{d\phi}{dk}$, respectively, in strongly-coupled systems, whereas they are intimately related in weakly-coupled ones. Therefore we search for a Λ that minimizes

$$\chi^2 = \frac{1}{2N} \sum_{k_{\rm F}} \left\{ \left(\frac{\Delta(k_{\rm F})_{\rm RMF} - \Delta(k_{\rm F})_{\rm Bonn}}{\Delta(k_{\rm F})_{\rm Bonn}} \right)^2 + \left(\frac{\xi_{\rm RMF} - \xi_{\rm Bonn}}{\xi_{\rm Bonn}} \right)^2 \right\} , \tag{3·10}$$

with $N = 11$ ($k_{\rm F} = 0.2, 0.3, ..., 1.2$ fm^{-1}). The obtained value is $\Lambda = 7.26$ fm^{-1}.[37] For consistency, we included the form factor also in the polarization diagrams, but it has almost no effect on them, because the polarization effectively involves only low momenta (see the following figures).

Equation (3·1) indicates that $V_{\rm RPA}$ becomes ill-defined when the liquid-gas instability occurs. This means that superfluidity in the liquid-gas coexistent phase rather than that in the liquid phase should be considered. However, in the present calculation, we consider the case in which the system remains in a pure phase also in the instability region (0.3 fm^{-1} $< k_{\rm F} <$ 1.3 fm^{-1} in the FD case), as usual. Therefore, in that region, only a qualitative treatment is possible. Reference 27) also mentioned the existence of the instability. Note that the treatment is quantitative in high and low density regions, which are free from the instability. Figure 4 shows the cross sections of the longitudinal and the transverse dielectric functions. Figure 4(a) is for $k_{\rm F} = 0.8$ fm^{-1} and (b) is for $k_{\rm F} = 1.4$ fm^{-1}. The former shows that a low momentum cutoff is necessary to regularize the calculation in the instability region. For this reason, we introduce $\epsilon_{\rm cut}$, which acts to cut $|\boldsymbol{q}|$ that satisfies the relation $\epsilon_{\rm L/T}(0, |\boldsymbol{q}|) \leq \epsilon_{\rm cut}$. Because other parameters were determined at the saturation density, we chose $\epsilon_{\rm cut} = 0.65$, which maintains the full variation of $\epsilon_{\rm L}$ and $\epsilon_{\rm T}$ around

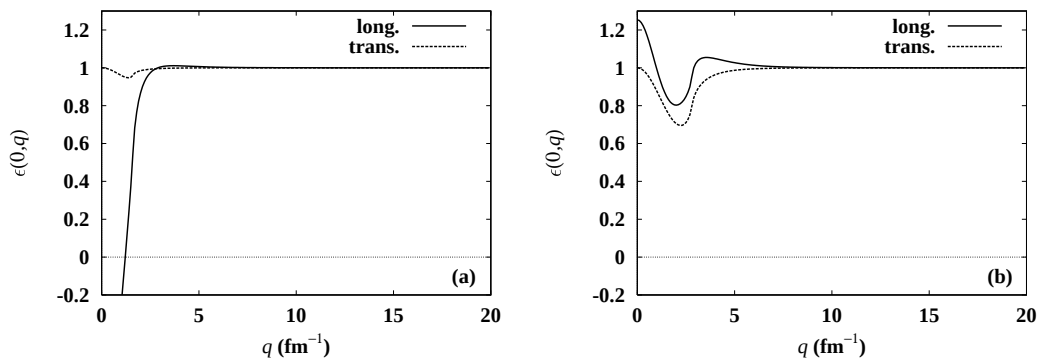

Fig. 4. Cross sections of the dielectric functions for the FD case of symmetric nuclear matter as functions of the momentum transfer: (a) $k_{\rm F} = 0.8$ fm^{-1}; (b) $k_{\rm F} = 1.4$ fm^{-1}.

this density (see Fig. 4(b)). This also serves to make the $k_{\rm F}$ dependence of $\Delta(k_{\rm F})$ smooth at the boundary of the instability region. Figure 5 plots the dependence of $\Delta(k_{\rm F} = 0.8\ {\rm fm}^{-1})$ on $\epsilon_{\rm cut}$. It is seen that its dependence is moderate around the chosen value. Figure 6 compares the gap $\Delta(k_{\rm F})$. This figure shows that the medium polarization increases the gap at all densities in the FD case. This result was also found in the previous calculation,[31] in which the form factor modulating the high momentum interaction was not introduced. Batista et al.,[26] who weakened the effect of the bubble diagram with their x parameter, obtained a similar result. The contents of the polarization interaction, $V_{\rm RPA} - V_{\rm OBE}$, are decomposed in Fig. 7. (The k dependence in Fig. 7(a) is a result of $\epsilon_{\rm cut}$ for q.) These figures reveal the characteristic feature that the σ polarization and the longitudinal ω polarization give strong attractions, whereas the σ-ω mixed polarization gives a strong repulsion, and they strongly cancel each other. The remaining tiny attraction leads to an increase of $\Delta(k_{\rm F})$. It is thus seen that the omission of the σ-ω mixed polarization in Ref. 25) would cause an imbalance. The transverse ω polarization, which represents the spin density fluctuation, is slightly repulsive, but the repulsion in the momentum region in which $\Delta(k) < 0$ (which is predominantly determined by $V_{\rm OBE}$) also increases $\Delta(k_{\rm F})$, because of the structure of the gap equation (3·4).

Figure 6 also displays the result for the pha case. The results for the FD and pha cases are very close to each other at low densities. This is because the particle propagation contained in $G_{\rm D}$ is small. However, their difference grows as the density increases; at high $k_{\rm F}$, the polarization reduces $\Delta(k_{\rm F})$, in contrast to the FD case. This is a result of the total polarization interaction becoming repulsive (Fig. 8).

Finally, we briefly mention the pure neutron matter case. It is yet unclear whether a liquid-gas instability exists for pure neutron matter. In the present calculations, it exists in the FD case. In the pha case, it does not exist but $\epsilon_{\rm L}$ strongly decreases at medium $k_{\rm F}$. Consequently, the behavior of $\Delta(k_{\rm F})$ is similar to that in the symmetric matter case (Fig. 9).

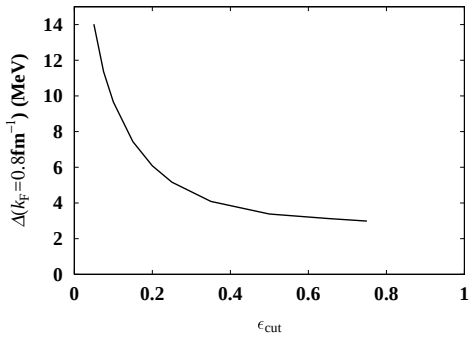

Fig. 5. Cutoff parameter dependence of $\Delta(k_{\rm F})$ at $k_{\rm F} = 0.8\ {\rm fm}^{-1}$.

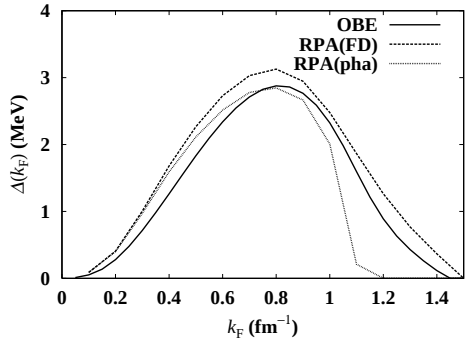

Fig. 6. Pairing gaps at the Fermi surface for symmetric nuclear matter as functions of the Fermi momentum.

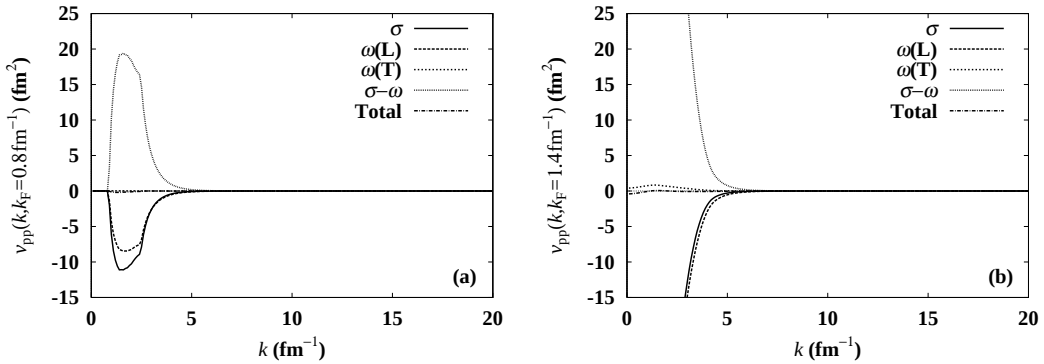

Fig. 7. Decomposition of the polarization interaction for the FD case of symmetric nuclear matter as functions of the momentum: (a) $k_{\rm F} = 0.8$ fm^{-1}; (b) $k_{\rm F} = 1.4$ fm^{-1}.

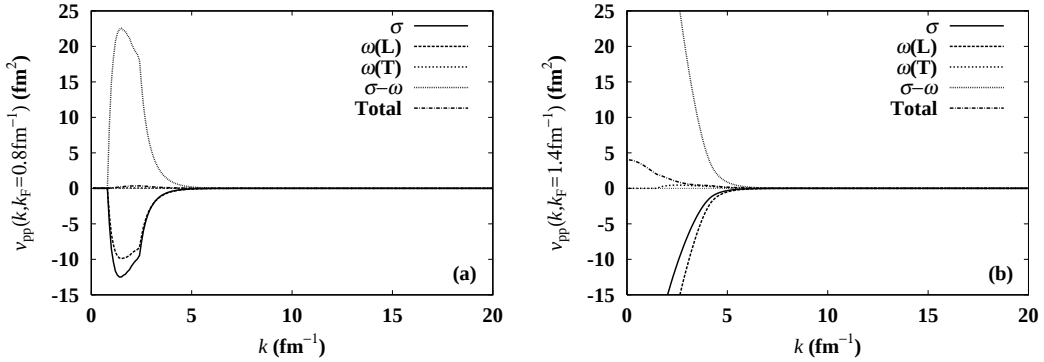

Fig. 8. The same as Fig. 7, but for the pha case.

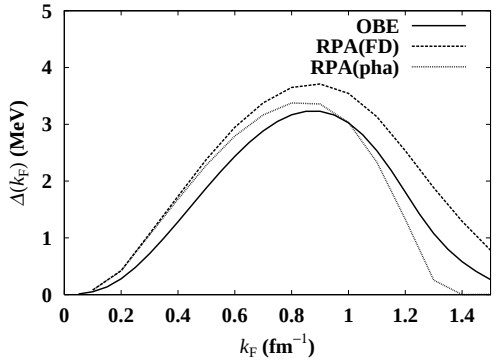

Fig. 9. The same as Fig. 6, but for pure neutron matter.

§4. Discussion and conclusion

In symmetric nuclear matter, the RPA predicts a liquid-gas instability at moderate densities even at zero temperature. Although the present study is restricted to zero temperature, the liquid-gas instability would produce an additional temperature

dependence of the pairing gap. In the present study, we concentrated on the medium polarization, but Ref. 28) showed that the liquid-gas instability survives even after inclusion of the vacuum polarization. This indicates that the polarization effects on superfluidity should be considered in the liquid-gas coexistent phase rather than in the liquid phase. In the present investigation, however, we have studied superfluidity in the liquid phase, as usual. Therefore, only a qualitative treatment could be carried out for the density region in which the instability appears. We found that the predicted gap is larger than the OBE result. In other regions, free from the instability, a quantitative treatment is possible. In those cases, it was found that the gap increases in the FD decomposition and decreases in the pha decomposition at high densities. At low densities, the gap increases in both cases. This behavior results from the characteristic cancellation between the attraction from the σ polarization and the longitudinal ω polarization and the repulsion from the σ-ω mixed polarization. The result for the FD case is consistent with that of another relativistic study presented in Ref. 26), and of a non-relativistic study presented in Ref. 27). The results in both cases are consistent with those of Ref. 19) as for the lowest density region. It is known that the coupling to surface vibrations enhances pairing in finite nuclei.[40)–42)] This tendency is in the same direction as in the FD case in the present calculation. However, because the polarization in the infinite matter case consists of density modes, their correspondence should be clarified.

It should be stressed that it is an approximation to consider only the medium (particle-hole) polarization in the relativistic model. For a more realistic treatment, the vacuum (particle-antiparticle) polarization should also be included. Because the gap is sensitive to the tiny part surviving the strong cancellation mentioned above, inclusion of the vacuum polarization is important. Answering the question of whether the FD or the pha decomposition is a better approximation of the full calculation is postponed until we are able to carry out an analysis including the vacuum polarization. This will be done in a later work. According to Refs. 43) and 44), the vacuum polarization leads to a decrease in the vector meson mass. In a previous paper,[45)] we examined this decrease using the in-medium Bonn potential and concluded that it reduces the gap.

It is not yet clear whether the liquid-gas instability exists in pure neutron matter. In the present calculation, it appears in the FD case. Although it does not appear in the pha case, the longitudinal dielectric function decreases strongly. Consequently, the results for the gap are similar to those in the symmetric matter case. Note that decrease of the Landau parameter F_0 to approximately -1 was reported in Ref. 27). In most non-relativistic calculations,[14)–22)] a decrease of the gap was reported. This is due to tha fact that the liquid-gas instability does not appear and to the repulsive effect of the spin density fluctuation. In the present model, the effect of the transverse ω polarization that corresponds to the spin density mode is weak. It is worth noting here that a recent *ab initio* calculation[23)] concluded that the polarization effect in pure neutron matter is weak.

From the point of view of many-body theory, higher-order diagrams, such as those studied by Babu and Brown,[46)] should be considered as an extension of the present study. Other ingredients that are not considered in the present study are the

inclusion of the exchange of other mesons, like π and ρ, and self-energy effects.[47)–49)] Study of superfluidity in the liquid-gas coexistent phase is also an interesting issue.

Acknowledgements

The author is grateful to Professor P. Ring for suggesting the problem and Professor H. Kouno for useful discussions.

Appendix A
—— *Medium Polarization Insertions* ——

A.1. *Feynman density decomposition*

In the Feynman density decomposition, we have the following:

$$\begin{aligned}\Pi^{\mathrm{S}} = \frac{2\lambda g_\sigma^2}{(2\pi)^2}\Big[& k_{\mathrm{F}}E_{\mathrm{F}}^* - \frac{1}{2}(6M^{*\,2}+|\boldsymbol{q}|^2)\ln\Big(\frac{k_{\mathrm{F}}+E_{\mathrm{F}}^*}{M^*}\Big) \\ & + \frac{4M^{*\,2}+|\boldsymbol{q}|^2}{4|\boldsymbol{q}|}\Big(2E_{\mathrm{F}}^* - \sqrt{4M^{*\,2}+|\boldsymbol{q}|^2}\Big)\ln\Big|\frac{|\boldsymbol{q}|-2k_{\mathrm{F}}}{|\boldsymbol{q}|+2k_{\mathrm{F}}}\Big| \\ & + \frac{(4M^{*\,2}+|\boldsymbol{q}|^2)^{3/2}}{4|\boldsymbol{q}|}\ln\Big|\frac{E_{\mathrm{F}}^*\sqrt{4M^{*\,2}+|\boldsymbol{q}|^2}+2M^{*\,2}+|\boldsymbol{q}|k_{\mathrm{F}}}{E_{\mathrm{F}}^*\sqrt{4M^{*\,2}+|\boldsymbol{q}|^2}+2M^{*\,2}-|\boldsymbol{q}|k_{\mathrm{F}}}\Big|\Big]\,, \end{aligned} \tag{A·1}$$

$$\begin{aligned}\Pi^{\mathrm{L}} = -\frac{2\lambda g_\omega^2}{(2\pi)^2}\Big[& \frac{4}{3}k_{\mathrm{F}}E_{\mathrm{F}}^* - \frac{1}{3}|\boldsymbol{q}|^2\ln\Big(\frac{k_{\mathrm{F}}+E_{\mathrm{F}}^*}{M^*}\Big) \\ & + \frac{1}{6|\boldsymbol{q}|}\Big(E_{\mathrm{F}}^*(3|\boldsymbol{q}|^2-4E_{\mathrm{F}}^{*\,2}) + (2M^{*\,2}-|\boldsymbol{q}|^2)\sqrt{4M^{*\,2}+|\boldsymbol{q}|^2}\Big)\ln\Big|\frac{|\boldsymbol{q}|-2k_{\mathrm{F}}}{|\boldsymbol{q}|+2k_{\mathrm{F}}}\Big| \\ & - \frac{1}{6|\boldsymbol{q}|}(2M^{*\,2}-|\boldsymbol{q}|^2)\sqrt{4M^{*\,2}+|\boldsymbol{q}|^2}\ln\Big|\frac{E_{\mathrm{F}}^*\sqrt{4M^{*\,2}+|\boldsymbol{q}|^2}+2M^{*\,2}+|\boldsymbol{q}|k_{\mathrm{F}}}{E_{\mathrm{F}}^*\sqrt{4M^{*\,2}+|\boldsymbol{q}|^2}+2M^{*\,2}-|\boldsymbol{q}|k_{\mathrm{F}}}\Big|\Big]\,, \end{aligned} \tag{A·2}$$

$$\begin{aligned}\Pi^{\mathrm{T}} = -\frac{2\lambda g_\omega^2}{(2\pi)^2}\Big[& -\frac{1}{3}k_{\mathrm{F}}E_{\mathrm{F}}^* + \frac{1}{3}|\boldsymbol{q}|^2\ln\Big(\frac{k_{\mathrm{F}}+E_{\mathrm{F}}^*}{M^*}\Big) \\ & - \frac{1}{6|\boldsymbol{q}|}\Big(E_{\mathrm{F}}^*\Big(2E_{\mathrm{F}}^{*\,2}-6M^{*\,2}+\frac{3}{2}|\boldsymbol{q}|^2\Big) + (2M^{*\,2}-|\boldsymbol{q}|^2)\sqrt{4M^{*\,2}+|\boldsymbol{q}|^2}\Big)\ln\Big|\frac{|\boldsymbol{q}|-2k_{\mathrm{F}}}{|\boldsymbol{q}|+2k_{\mathrm{F}}}\Big| \\ & + \frac{1}{6|\boldsymbol{q}|}(2M^{*\,2}-|\boldsymbol{q}|^2)\sqrt{4M^{*\,2}+|\boldsymbol{q}|^2}\ln\Big|\frac{E_{\mathrm{F}}^*\sqrt{4M^{*\,2}+|\boldsymbol{q}|^2}+2M^{*\,2}+|\boldsymbol{q}|k_{\mathrm{F}}}{E_{\mathrm{F}}^*\sqrt{4M^{*\,2}+|\boldsymbol{q}|^2}+2M^{*\,2}-|\boldsymbol{q}|k_{\mathrm{F}}}\Big|\Big]\,, \end{aligned} \tag{A·3}$$

$$\Pi^0 = \frac{2\lambda g_\sigma g_\omega}{(2\pi)^2}M^*\Big[k_{\mathrm{F}} + \frac{|\boldsymbol{q}|^2-4k_{\mathrm{F}}^2}{4|\boldsymbol{q}|}\ln\Big|\frac{|\boldsymbol{q}|-2k_{\mathrm{F}}}{|\boldsymbol{q}|+2k_{\mathrm{F}}}\Big|\Big]\,. \tag{A·4}$$

A.2. *Particle-hole-antiparticle decomposition*

In the particle-hole-antiparticle decomposition, we have the following:

$$
\begin{aligned}
\Pi^{\mathrm{S}} = \frac{2\lambda g_\sigma^2}{(2\pi)^2}\Big[&\frac{1}{2}k_{\mathrm{F}}E_{\mathrm{F}}^* - \frac{1}{4}(6M^{*\,2}+|\boldsymbol{q}|^2)\ln\Big(\frac{k_{\mathrm{F}}+E_{\mathrm{F}}^*}{M^*}\Big)\\
-\frac{(4M^{*\,2}+|\boldsymbol{q}|^2)^{3/2}}{8|\boldsymbol{q}|}&\Big(2\ln\Big|\frac{|\boldsymbol{q}|-2k_{\mathrm{F}}}{|\boldsymbol{q}|+2k_{\mathrm{F}}}\Big| - \ln\Big|\frac{E_{\mathrm{F}}^*\sqrt{4M^{*\,2}+|\boldsymbol{q}|^2}+2M^{*\,2}+|\boldsymbol{q}|k_{\mathrm{F}}}{E_{\mathrm{F}}^*\sqrt{4M^{*\,2}+|\boldsymbol{q}|^2}+2M^{*\,2}-|\boldsymbol{q}|k_{\mathrm{F}}}\Big|\\
&+\ln\Big|\frac{\mathcal{E}_+\sqrt{4M^{*\,2}+|\boldsymbol{q}|^2}+2M^{*\,2}+|\boldsymbol{q}|^2+|\boldsymbol{q}|k_{\mathrm{F}}}{\mathcal{E}_-\sqrt{4M^{*\,2}+|\boldsymbol{q}|^2}+2M^{*\,2}+|\boldsymbol{q}|^2-|\boldsymbol{q}|k_{\mathrm{F}}}\Big|\Big)\\
-\frac{1}{6|\boldsymbol{q}|}&\Big(\mathcal{E}_+^3-\mathcal{E}_-^3\Big)+\frac{1}{4}k_{\mathrm{F}}\Big(\mathcal{E}_++\mathcal{E}_-\Big)-\frac{M^{*\,2}}{|\boldsymbol{q}|}\Big(\mathcal{E}_+-\mathcal{E}_-\Big)\\
&-\frac{E_{\mathrm{F}}^*}{2|\boldsymbol{q}|}(4M^{*\,2}+|\boldsymbol{q}|^2)\ln\Big|\frac{\mathcal{E}_+-E_{\mathrm{F}}^*}{\mathcal{E}_--E_{\mathrm{F}}^*}\Big|\\
&+\frac{1}{8}(6M^{*\,2}+|\boldsymbol{q}|^2)\ln\Big|\frac{\big(\mathcal{E}_++k_{\mathrm{F}}+|\boldsymbol{q}|\big)\big(\mathcal{E}_-+k_{\mathrm{F}}-|\boldsymbol{q}|\big)}{M^{*\,2}}\Big|\Big]\,,
\end{aligned}
\tag{A·5}
$$

$$
\begin{aligned}
\Pi^{\mathrm{L}} = -\frac{2\lambda g_\omega^2}{(2\pi)^2}\Big[&\frac{2}{3}k_{\mathrm{F}}E_{\mathrm{F}}^* - \frac{1}{6}|\boldsymbol{q}|^2\ln\Big(\frac{k_{\mathrm{F}}+E_{\mathrm{F}}^*}{M^*}\Big)\\
+\frac{1}{12|\boldsymbol{q}|}&(2M^{*\,2}-|\boldsymbol{q}|^2)\sqrt{4M^{*\,2}+|\boldsymbol{q}|^2}\Big(2\ln\Big|\frac{|\boldsymbol{q}|-2k_{\mathrm{F}}}{|\boldsymbol{q}|+2k_{\mathrm{F}}}\Big|\\
&-\ln\Big|\frac{E_{\mathrm{F}}^*\sqrt{4M^{*\,2}+|\boldsymbol{q}|^2}+2M^{*\,2}+|\boldsymbol{q}|k_{\mathrm{F}}}{E_{\mathrm{F}}^*\sqrt{4M^{*\,2}+|\boldsymbol{q}|^2}+2M^{*\,2}-|\boldsymbol{q}|k_{\mathrm{F}}}\Big|\\
&+\ln\Big|\frac{\mathcal{E}_+\sqrt{4M^{*\,2}+|\boldsymbol{q}|^2}+2M^{*\,2}+|\boldsymbol{q}|^2+|\boldsymbol{q}|k_{\mathrm{F}}}{\mathcal{E}_-\sqrt{4M^{*\,2}+|\boldsymbol{q}|^2}+2M^{*\,2}+|\boldsymbol{q}|^2-|\boldsymbol{q}|k_{\mathrm{F}}}\Big|\Big)\\
+\frac{1}{15|\boldsymbol{q}|^3}&\Big(\mathcal{E}_+^5-\mathcal{E}_-^5\Big)-\frac{k_{\mathrm{F}}}{3|\boldsymbol{q}|^2}\Big(\mathcal{E}_+^3+\mathcal{E}_-^3\Big)\\
+\frac{11}{18|\boldsymbol{q}|}&\Big(\mathcal{E}_+^3-\mathcal{E}_-^3\Big)-\frac{7}{6}k_{\mathrm{F}}\Big(\mathcal{E}_++\mathcal{E}_-\Big)-\frac{2M^{*\,2}+5|\boldsymbol{q}|^2}{6|\boldsymbol{q}|}\Big(\mathcal{E}_+-\mathcal{E}_-\Big)\\
&+\frac{E_{\mathrm{F}}^*}{6|\boldsymbol{q}|}(4E_{\mathrm{F}}^{*\,2}-3|\boldsymbol{q}|^2)\ln\Big|\frac{\mathcal{E}_+-E_{\mathrm{F}}^*}{\mathcal{E}_--E_{\mathrm{F}}^*}\Big|\\
&+\frac{1}{12}|\boldsymbol{q}|^2\ln\Big|\frac{\big(\mathcal{E}_++k_{\mathrm{F}}+|\boldsymbol{q}|\big)\big(\mathcal{E}_-+k_{\mathrm{F}}-|\boldsymbol{q}|\big)}{M^{*\,2}}\Big|\Big]\,,
\end{aligned}
\tag{A·6}
$$

$$
\begin{aligned}
\Pi^{\mathrm{T}} = -\frac{2\lambda g_\omega^2}{(2\pi)^2}\Big[&-\frac{1}{6}k_{\mathrm{F}}E_{\mathrm{F}}^* + \frac{1}{6}|\boldsymbol{q}|^2\ln\Big(\frac{k_{\mathrm{F}}+E_{\mathrm{F}}^*}{M^*}\Big)\\
-\frac{1}{12|\boldsymbol{q}|}&(2M^{*\,2}-|\boldsymbol{q}|^2)\sqrt{4M^{*\,2}+|\boldsymbol{q}|^2}\Big(2\ln\Big|\frac{|\boldsymbol{q}|-2k_{\mathrm{F}}}{|\boldsymbol{q}|+2k_{\mathrm{F}}}\Big|\\
&-\ln\Big|\frac{E_{\mathrm{F}}^*\sqrt{4M^{*\,2}+|\boldsymbol{q}|^2}+2M^{*\,2}+|\boldsymbol{q}|k_{\mathrm{F}}}{E_{\mathrm{F}}^*\sqrt{4M^{*\,2}+|\boldsymbol{q}|^2}+2M^{*\,2}-|\boldsymbol{q}|k_{\mathrm{F}}}\Big|\\
&+\ln\Big|\frac{\mathcal{E}_+\sqrt{4M^{*\,2}+|\boldsymbol{q}|^2}+2M^{*\,2}+|\boldsymbol{q}|^2+|\boldsymbol{q}|k_{\mathrm{F}}}{\mathcal{E}_-\sqrt{4M^{*\,2}+|\boldsymbol{q}|^2}+2M^{*\,2}+|\boldsymbol{q}|^2-|\boldsymbol{q}|k_{\mathrm{F}}}\Big|\Big)
\end{aligned}
$$

$$
\begin{aligned}
&+\frac{1}{30|\boldsymbol{q}|^3}\Big(\mathcal{E}_+^5-\mathcal{E}_-^5\Big)-\frac{k_{\rm F}}{6|\boldsymbol{q}|^2}\Big(\mathcal{E}_+^3+\mathcal{E}_-^3\Big)\\
&+\frac{17}{36|\boldsymbol{q}|}\Big(\mathcal{E}_+^3-\mathcal{E}_-^3\Big)-\frac{5}{6}k_{\rm F}\Big(\mathcal{E}_++\mathcal{E}_-\Big)-\frac{8M^{*\,2}+5|\boldsymbol{q}|^2}{12|\boldsymbol{q}|}\Big(\mathcal{E}_+-\mathcal{E}_-\Big)\\
&+\frac{E_{\rm F}^*}{12|\boldsymbol{q}|}(4k_{\rm F}^2-8M^{*\,2}+3|\boldsymbol{q}|^2)\ln\Big|\frac{\mathcal{E}_+-E_{\rm F}^*}{\mathcal{E}_--E_{\rm F}^*}\Big|\\
&-\frac{1}{12}|\boldsymbol{q}|^2\ln\Big|\frac{\big(\mathcal{E}_++k_{\rm F}+|\boldsymbol{q}|\big)\big(\mathcal{E}_-+k_{\rm F}-|\boldsymbol{q}|\big)}{M^{*\,2}}\Big|\Big]\,,
\end{aligned}
\tag{A·7}
$$

$$
\begin{aligned}
\Pi^0=\frac{2\lambda g_\sigma g_\omega}{(2\pi)^2}M^*\Big[&\frac{1}{2}k_{\rm F}-\frac{|\boldsymbol{q}|^2-4k_{\rm F}^2}{4|\boldsymbol{q}|}\ln\Big|\frac{\mathcal{E}_+-E_{\rm F}^*}{\mathcal{E}_--E_{\rm F}^*}\Big|\\
&+\frac{3E_{\rm F}^*}{4|\boldsymbol{q}|}\Big(\mathcal{E}_+-\mathcal{E}_-\Big)\\
&+\frac{M^{*\,2}}{2|\boldsymbol{q}|}\ln\Big|\frac{\big(\mathcal{E}_+-E_{\rm F}^*-|\boldsymbol{q}|\big)\big(\mathcal{E}_+-E_{\rm F}^*+|\boldsymbol{q}|\big)}{\big(\mathcal{E}_--E_{\rm F}^*-|\boldsymbol{q}|\big)\big(\mathcal{E}_--E_{\rm F}^*+|\boldsymbol{q}|\big)}\Big|\Big]\,.
\end{aligned}
\tag{A·8}
$$

Here, we use the definition

$$
\mathcal{E}_\pm\equiv\sqrt{(k_{\rm F}\pm|\boldsymbol{q}|)^2+M^{*\,2}}\,. \tag{A·9}
$$

References

1) T. Takatsuka and R. Tamagaki, Prog. Theor. Phys. Suppl. No. 112 (1993), 27.
2) H.-P. Duerr, Phys. Rev. **103** (1956), 469.
3) M. H. Jhonson and E. Teller, Phys. Rev. **98** (1955), 783.
4) S. A. Chin and J. D. Walecka, Phys. Lett. B **52** (1974), 24.
5) J. D. Walecka, Ann. of Phys. **83** (1974), 491.
6) S. A. Chin, Ann. of Phys. **108** (1977), 301.
7) P. Ring, Prog. Part. Nucl. Phys. **37** (1996), 193.
8) B. D. Serot and J. D. Walecka, Int. J. Mod. Phys. E **6** (1997), 515.
9) A. B. Migdal, *Theory of Finite Fermi Systems and Applications to Atomic Nuclei* (Wiley, New York, 1967).
10) M. Baldo, J. Cugnon, A. Lejeune and U. Lombardo, Nucl. Phys. A **515** (1990), 409.
11) L. N. Cooper, R. L. Mills and A. M. Sessler, Phys. Rev. **114** (1959), 1377.
12) T. Marumori, T. Muroya, S. Takagi, H. Tanaka and M. Yasuno, Prog. Theor. Phys. **25** (1961), 1035.
13) G. F. Bertsch and H. Esbensen, Ann. of Phys. **209** (1991), 327.
14) J. W. Clark, C.-G. Källman, C.-H. Yang and D. A. Chakkalakal, Phys. Lett. B **61** (1976), 331.
15) J. M. C. Chen, J. W. Clark, E. Krotscheck and R. A. Smith, Nucl. Phys. A **451** (1986), 509.
16) T. L. Ainsworth, J. Wambach and D. Pines, Phys. Lett. B **222** (1989), 173.
17) J. Wambach, T. L. Ainsworth and D. Pines, Nucl. Phys. A **555** (1993), 128.
18) H.-J. Schulze, J. Cugnon, A. Lejeune, M. Baldo and U. Lombardo, Phys. Lett. B **375** (1996), 1.
19) H. Heiselberg, C. J. Pethick, H. Smith and L. Viverit, Phys. Rev. Lett. **85** (2000), 2418.
20) H.-J. Schulze, A. Polls and A. Ramos, Phys. Rev. C **63** (2001), 044310.
21) C. Shen, U. Lombardo, P. Schuck, W. Zuo and N. Sandulescu, Phys. Rev. C **67** (2003), 061302(R).
22) A. Schwenk, B. Friman and G. E. Brown, Nucl. Phys. A **713** (2003), 191.

23) A. Fabrocini, S. Fantoni, A. Yu. Illarionov and K. A. Schmidt, Phys. Rev. Lett. **95** (2005), 192501.
24) U. Lombardo, P. Schuck and C. Shen, Nucl. Phys. A **731** (2004), 392.
25) J.-S. Chen, P.-F. Zhuang and J.-R. Li, Phys. Lett. B **585** (2004), 85.
26) E. F. Batista, B. V. Carlson and T. Frederico, Nucl. Phys. A **765** (2006), 75.
27) C. Shen, U. Lombardo and P. Schuck, Phys. Rev. C **71** (2005), 054301.
28) B. L. Friman and P. A. Henning, Phys. Lett. B **206** (1988), 579.
29) R. J. Furnstahl and C. J. Horowitz, Nucl. Phys. A **485** (1988), 632.
30) K. Lim and C. J. Horowitz, Nucl. Phys. A **501** (1989), 729.
31) M. Matsuzaki and P. Ring, in *Proc. APCTP Workshop on Astro-Hadron Physics in Honor of Prof. Mannque Rho's 60th Birthday: Properties of Hadrons in Matter,* ed. G. E. Brown, C.-H. Lee, H. K. Lee and D.-P. Min (World Scientific, Singapore, 1999), p. 243; nucl-th/9712060.
32) H. Kurasawa and T. Suzuki, Nucl. Phys. A **445** (1985), 685.
33) B. D. Serot and J. D. Walecka, Adv. Nucl. Phys. **16** (1986), 1.
34) M. Nakano, N. Noda, T. Mitsumori, K. Koide, H. Kouno, A. Hasegawa and L.-G. Liu, Phys. Rev. C **56** (1997), 3287.
35) H. Kucharek and P. Ring, Z. Phys. A **339** (1991), 23.
36) M. Matsuzaki, Phys. Rev. C **58** (1998), 3407.
37) M. Matsuzaki and T. Tanigawa, Nucl. Phys. A **683** (2001), 406.
38) T. Tanigawa and M. Matsuzaki, Prog. Theor. Phys. **102** (1999), 897.
39) R. Machleidt, Adv. Nucl. Phys. **19** (1989), 189.
40) F. Barranco, R. A. Broglia, G. Gori, E. Vigezzi, P. F. Bortignon and J. Terasaki, Phys. Rev. Lett. **83** (1999), 2147.
41) J. Terasaki, F. Barranco, R. A. Broglia, E. Vigezzi and P. F. Bortignon, Nucl. Phys. A **697** (2002), 127.
42) G. Gori, F. Ramponi, F. Barranco, P. F. Bortignon, R. A. Broglia, G. Colò and E. Vigezzi, Phys. Rev. C **72** (2005), 011302(R).
43) H.-C. Jean, J. Piekarewicz and A. G. Williams, Phys. Rev. C **49** (1994), 1981.
44) T. Hatsuda, H. Shiomi and H. Kuwabara, Prog. Theor. Phys. **95** (1996), 1009.
45) M. Matsuzaki and T. Tanigawa, Phys. Lett. B **445** (1999), 254.
46) S. Babu and G. E. Brown, Ann. of Phys. **78** (1973), 1.
47) P. Bożek, Nucl. Phys. A **657** (1999), 187.
48) M. Baldo and A. Grasso, Phys. Lett. B **485** (2000), 115.
49) U. Lombardo, P. Schuck and W. Zuo, Phys. Rev. C **64** (2001), 021301(R).